

Ionization-induced enhancement of hydrogen storage in metalized C_2H_4 and C_5H_5 molecules

C. S. Liu* and Z. Zeng†

Key Laboratory of Materials Physics, Institute of Solid State Physics,
Chinese Academy of Sciences, Hefei 230031, People's Republic of China

and Graduate School of the Chinese Academy of Sciences, Beijing 100094, People's Republic of China

(Received 4 December 2008; revised manuscript received 13 March 2009; published 15 June 2009)

The capacity of $Li_2C_2H_4^+$ and $TiC_5H_5^+$ as hydrogen storage media is studied using first-principles density-functional theory. The present results indicate that these complexes not only enhance the metal bond strength but also increase the number of nondissociative hydrogen molecules attached. The adsorption capacity of $Li_2C_2H_4^+$ (27.5 wt %) is doubled compared with that of $Li_2C_2H_4$. The enhanced electrostatic field around the Li atom originating from the increased charge transfers from Li to $C_2H_4^+$ accounts for the high capacity. For $TiC_5H_5^+$, the first H_2 is adsorbed in molecular form, while it is adsorbed dissociatively on the TiC_5H_5 complex. This is due to the favorable overlap of the highest occupied molecular orbital of Ti and the lowest unoccupied molecular orbital of H_2 . Furthermore, the number of adsorbed H_2 on TiC_5H_5 is limited to only four, whereas the number increases to five on $TiC_5H_5^+$. The availability of the d_{z^2} orbital of Ti in $TiC_5H_5^+$ has been found to be responsible for the fifth H_2 adsorption with a hydrogen uptake of 8.1 wt %. It is demonstrated that controlling the charge state of the metal-organic molecules may play a significant role in the search for hydrogen storage media.

DOI: 10.1103/PhysRevB.79.245419

PACS number(s): 68.43.Bc, 71.15.Mb, 73.22.-f, 84.60.Ve

I. INTRODUCTION

Recently, the search for the promising hydrogen storage media has attracted increased attention.¹⁻⁵ The (U.S.) Department of Energy target for the ideal hydrogen storage material is that the gravimetric storage capacity of hydrogen should reach 9 wt % by 2015.⁶ Although much effort has been devoted to the design and study of novel materials with the aid of high-performance supercomputers and sophisticated quantum-mechanical method, the main obstacles lie in poor reversibility and low-gravimetric storage capacity under ambient conditions.⁷

Recently, carbon-based nanostructures have been the focus of intensive studies in many areas due to their light weight and many interesting properties. In particular, organometallic molecules based on fullerenes (especially C_{60}) have been widely studied for their application in hydrogen storage.⁸⁻¹⁴ C_{60} spheres coated with transition metals (TMs) have been found to be able to store large quantities of hydrogen. However it has been found that most TM atoms tended to form clusters on the surface of the C_{60} .¹³ On the other hand, alkali metals such as Li can coat uniformly due to the cohesive energy of Li being substantially smaller than that of transition metals. Hydrogen molecule physisorption, however, is rather weak with a binding energy of only a few meV/ H_2 , well below the ideal energy window of 0.2 ~ 0.6 eV. A very recent study¹⁵ has shown that Ca is superior to all metallic-coating elements on C_{60} suggested so far. $Ca_{32}C_{60}$ gives rise to high electric fields ($\sim 2.4 \times 10^{10}$ V/m) and shows a hydrogen uptake of >8.4 wt %. In addition, derivatives of C_{60} , such as C_2H_4 (Ref. 16) and C_5H_5 ,^{17,18} have been predicted to be potential bases for high-capacity hydrogen storage due to the C=C bond and cyclopentadiene ring mimicking similar structures in C_{60} that bind light-metal atoms. Calculations have shown that the ethylene molecule should be able to complex with two Li atoms (via

an electrostatic mechanism) and with two TM atoms (via Dewar coordination) (Ref. 19) reaching hydrogen adsorption capacities of 16 and 14 wt %, respectively.

On the experimental side, a $Li_2C_2H_4$ complex successfully formed by laser ablation exhibited 12 wt % uptake of H_2 with rapid kinetics at room temperature.²⁰ However, each Li and Ti atom could bind only two and four hydrogen molecules in $Li_2C_2H_4$ and TiC_5H_5 , respectively. This is in clear contrast to isolated Li^+ and Ti^+ atoms which can bind at least 12 hydrogen atoms in molecular form.⁹

In this paper, we show that $Li_2C_2H_4^+$ and $TiC_5H_5^+$ complexes can improve the capability of hydrogen storage. First, due to more valence electrons transfer from metal atoms to the charged templates, the bond strength between the Li (Ti) atom and the $C_2H_4^+$ ($C_5H_5^+$) template is enhanced. Second, according to the mechanism of the metal- H_2 interaction, i.e., Kubas²¹ or electrostatic interaction, the maximum number of hydrogen molecules adsorbed is determined by the intensity of the electrostatic field and the 18-electron rule.²² The ionic processes, by enhancing the degree of polarization of the Li atom and by reducing the number of electrons in the TiC_5H_5 system, would lead to higher capacity for H_2 molecule adsorption. In the current work, we have not considered the overall charge neutrality of the materials used for adsorbing hydrogen since our intention is to understand the mechanisms of adsorption. Clearly, charge neutrality would be a consideration in the engineering of practical materials for hydrogen storage.

II. COMPUTATIONAL DETAILS

The numerical calculations were performed using all-electron density-functional theory (DFT) at the level of the generalized gradient approximation (GGA) (Refs. 23 and 24) using the Perdew-Burke-Ernzerhof²⁵ exchange-correlation functional. A double numerical-polarized (DNP) (Ref. 26)

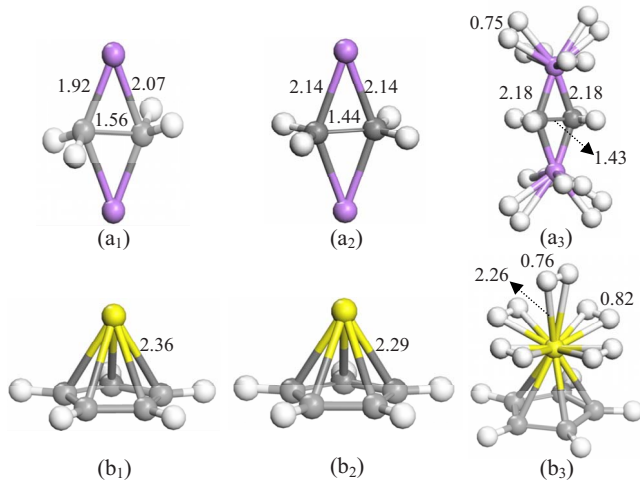


FIG. 1. (Color online) Optimized geometries of (a₁) Li₂C₂H₄, (a₂) Li₂C₂H₄⁺, (a₃) Li₂C₂H₄⁺(H₂)₈, (b₁) TiC₅H₅, (b₂) TiC₅H₅⁺, and (b₃) TiC₅H₅⁺(H₂)₅ along with important bond lengths (Å).

basis set that includes all occupied atomic orbitals plus a second set of valence atomic orbitals plus polarized *d*-valence orbitals was employed. In the self-consistent-field calculations, the electronic-density convergence was set to $1 \times 10^{-6} e/\text{Å}^3$. The convergence criteria during geometry optimization were 10^{-5} Hartree for the energy, 2×10^{-3} Hartree/Å for the force, and 10^{-4} Å for atomic displacements. For all the obtained structures, we performed normal-mode analysis to check whether the structures optimized without any symmetry constraints were true minima on the potential-energy surface. To test the validity of the above convergence parameters, the calculated properties of neutral and charged ethylene molecules have been compared with previous work. The three main vibrational normal modes, CH₂ wag (934 cm⁻¹) and CH₂ stretch (3146 and 3249 cm⁻¹), were in satisfactory agreement with the experimental results:²⁷ 949, 2989, and 3105 cm⁻¹, respectively. The ground-state geometric configuration of C₂H₄⁺ was found to include a twist with an angle of 36.5°, which has been predicted by theoretical studies and confirmed experimentally.^{28,29} The ionization potential, the energy difference between the optimized neutral C₂H₄ and its positively charged counterpart, was 10.3 eV in accord with the experimental result of 10.5 eV.³⁰ All computations are implemented in the DMOL³ package (Accelrys Inc.).³¹

III. RESULTS AND DISCUSSIONS

A. Configurations and electronic structures of Li₂C₂H₄⁺ and TiC₅H₅⁺

We first optimized the equilibrium structures of Li-coated C₂H₄⁺ and Ti-coated C₅H₅⁺ as shown in Fig. 1. It has been found that each Li atom is bound to two C atoms at two distances (1.92 and 2.07 Å) in Li₂C₂H₄ [Fig. 1, (a₁)], whereas all Li-C bond lengths (2.14 Å) are equal in Li₂C₂H₄⁺ [Fig. 1, (a₂)]. The average Ti-C bond length in TiC₅H₅⁺ is about 2.29 Å [Fig. 1, (b₂)], which is slightly shorter than that of TiC₅H₅ (2.36 Å) [Fig. 1, (b₁)]. In order

to evaluate the stability, we calculated the binding energy (E_b) for the reaction channel $T+M \rightarrow C$ [$T=C_2H_4$ (C₅H₅⁺), $M=Li_2(Ti)$, and $C=Li_2C_2H_4^+(TiC_5H_5^+)$] using the expression

$$E_b(M) = [E_T + E_M - E_C]/n, \quad (1)$$

where E_T , E_M , E_C , and n represent the total energy of T , M , C , and the number of metal atoms, respectively. The binding energy of the Ti atom to C₅H₅⁺ was found to be 7.02 eV which is significantly larger than the cohesive energy of bulk Ti (3.68 eV). However, the Ti atom was found to bind to C₅H₅ with E_b of only 3.98 eV.¹⁷ Thus the stability of TiC₅H₅⁺ is assured. In the case of Li₂C₂H₄⁺, the average binding energy of each Li (3.73 eV) was much larger than that of Li in Li₂C₂H₄ (0.69 eV).¹⁶ From the above results, it may be seen that the metal atoms are bound strongly to the templates and are therefore prevented from clustering, suggesting that the storage medium should be stable.

The electronic structures for both neutral and charged C₂H₄, C₅H₅, Li₂C₂H₄, and TiC₅H₅ were analyzed by studying the highest occupied molecular orbital (HOMO), lowest unoccupied molecular orbital (LUMO), and energy levels around the Fermi level. In Fig. 2, since the metal atoms are bound to neutral templates, the HOMO-LUMO gap, as shown in Fig. 2 [(a₂) or (b₂)], is not only reduced compared with that of neutral templates [Fig. 2, (a₁) or (b₁)] but the interactions between the metal atom and the template also change the energy-level distribution. Comparison of the energy levels of C₂H₄ (C₅H₅) with those of C₂H₄⁺ (C₅H₅⁺) in Fig. 1 shows that the most pronounced effect of replacing the neutral system with the corresponding charged one is a significant lowering of the electron energy levels. In addition, the energy levels of Li₂C₂H₄⁺(TiC₅H₅⁺) shift upward relative to those of C₂H₄⁺(C₅H₅⁺). This shift is larger than that between Li₂C₂H₄(TiC₅H₅) and C₂H₄(C₅H₅), suggesting a stronger interaction between the metal atoms and charged templates. Analysis of molecular-orbital coefficients for the neutral Li₂C₂H₄ complex shows that the HOMO comes from the hybridized *2p* orbital of Li and the π^* antibonding orbital of C₂H₄. Likewise, the main contributions to the LUMO are the *2s-2p_z* hybridization of Li and the *2s-2p_x* hybridization of C. On the other hand, for C₂H₄⁺, the HOMO appears as a mixture including $\sim 50\%$ from orbitals of H atoms and the rest from *2p_y* and *2p_z* orbitals of C atoms. The components of the LUMO are similar to those of the HOMO, except that the *s* orbitals of H atoms contribute $\sim 12\%$, suggesting that in the next growth stage the incoming Li atoms will bind with the template through *2p* electron transfer. In fact, the Mulliken charge analysis demonstrates that about 0.8 electrons are transferred from Li to C₂H₄⁺, indicating the bond feature has significant ionic character. Essentially, the bonding orbital for the TM atoms and C₅H₅ results from the hybridization of the lowest unoccupied molecular orbital of the C₅H₅ and the TM *d* orbitals, in accord with Dewar coordination.²² In the TiC₅H₅ complex, charge is transferred from the metal atom to the organic molecule owing to the electron deficiency of C₅H₅. Among the five *d* orbitals of Ti, only three orbitals, i.e., *d_{zx}*, *d_{yz}*, and *d_{z2}*, have the right symmetry to interact with the π orbital of the complex. In Fig. 2 (b₂), the HOMO shows the hybridization of a linear combi-

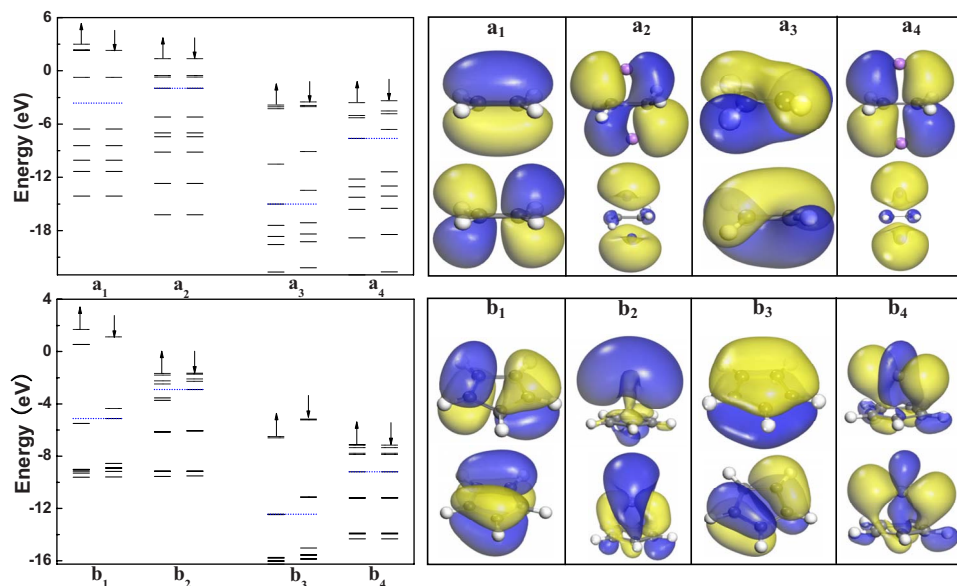


FIG. 2. (Color online) The left panels show energy levels for the ground state of (a₁) C₂H₄, (a₂) Li₂C₂H₄, (a₃) C₂H₄⁺, (a₄) Li₂C₂H₄⁺, (b₁) C₅H₅, (b₂) TiC₅H₅, (b₃) C₅H₅⁺, and (b₄) TiC₅H₅⁺. The solid lines refer to occupied states and the dotted lines refer to unoccupied states. The blue dotted lines indicate the Fermi energy for the respective energy levels. For each system, two level diagrams are given. The arrow denotes the spin state: up for the spin-up state and down for the spin-down state. The HOMO and LUMO correspond to the smaller HOMO-LUMO-gap value in the individual gaps for the spin-up and spin-down states. The right panels show the corresponding electron density of the HOMO and LUMO orbitals at an isovalue of 0.02 e/Å³.

nation of $4s$, $3d_{xy}$, and $3d_{yz}$ with the π orbital of C₅H₅, and the LUMO shows hybridization of the $3d_{z^2}$ with $3d_{xy}$. However, Ti interacts differently with C₅H₅⁺, owing to the reduced π electron. The HOMO in Fig. 2 (b₄) illustrates the hybridization of $3d_{xy}$ and $3d_{yz}$ with the orbital of C₅H₅⁺. The Ti- $4s$ orbital can hardly be seen due to its electron being partly transferred to C₅H₅⁺. The LUMO exhibits hybridization of t_{2g} orbitals ($3d_{xy}$, $3d_{yz}$, and $3d_{zx}$) with the orbitals of C₅H₅⁺.

B. Hydrogen adsorption on Li₂C₂H₄⁺

The first H₂ introduced into the Li₂C₂H₄⁺ system remains in the form of a dihydrogen molecule due to the polarization interaction between the charged Li atom and the H₂. The H-H bond length expands slightly from 0.74 to 0.76 Å and the equilibrium Li-H distance is found to be 2.03 Å, which is very close to the value (2.04 Å) found in the case of a free Li⁺ ion interacting with H₂.³² In the presence of H₂, the Li-C distances change from 2.14 Å to 2.15 Å. The C-C bond length (1.44 Å) in the Li₂C₂H₄⁺(H₂) is close to that in neutral C₂H₄. As the number of adsorbed H₂ molecules increases, the extent of bond-length elongation of H₂ decreases slightly. Optimized geometries for the Li₂C₂H₄⁺(H₂)₈ complex are sketched in Fig. 1 (a₃). In contrast to the Li₂C₂H₄(H₂)₄ system, we can now add eight H₂ molecules to the Li₂C₂H₄⁺ for an adsorption capacity of 27.5 wt %. All the H-H bond lengths of the H₂ molecules are 0.75 Å. When the ninth H₂ is attached to Li₂C₂H₄⁺(H₂)₈, the separation distance between the Li and the H₂ molecule increases to 4.2 Å suggesting that the ninth H₂ molecule may not be useful as far as hydrogen storage is concerned.

To understand the reason that Li atom can adsorb eight H₂ molecules, we now turn to an electronic-structure analysis of

the system. The Li-H₂ interaction is easy to understand as an electrostatic interaction. To give a more detailed account of the effects induced by the charge distribution, we show in Fig. 3 a two-dimensional potential energy contour plot of the all-electron electrostatic potential energy calculated for Li₂C₂H₄ and Li₂C₂H₄⁺. The different potential energies between the two cases show that the enhanced electric field around the Li atom in Li₂C₂H₄⁺ causes other H₂ molecules to be adsorbed. Yoon *et al.*¹⁵ also expressed the view that the charge redistribution gives rise to large electric fields surrounding the coated fullerenes.

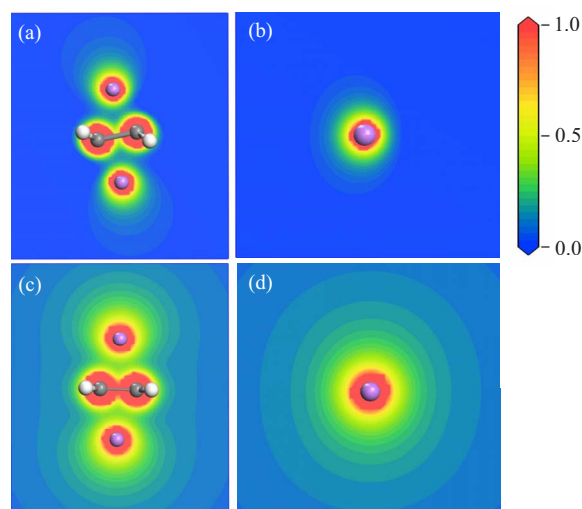


FIG. 3. (Color online) Planar contour plots of the all-electron electrostatic potential energy of Li₂C₂H₄ (panel a and panel b) and Li₂C₂H₄⁺ (panel c and panel d). The potential energy is lowest (highest) in the blue (red) regions.

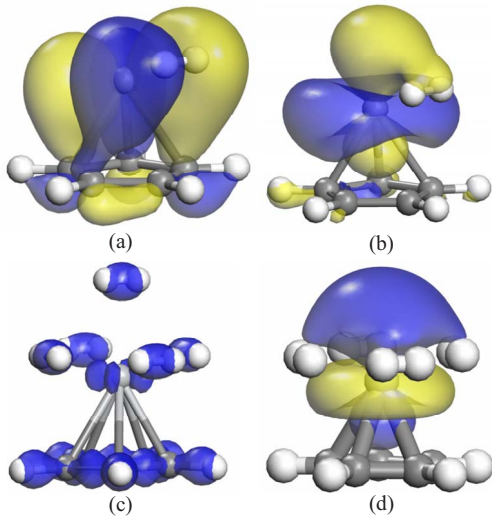


FIG. 4. (Color online) The HOMO (a) and LUMO (b) orbitals of the first hydrogen molecules adsorbed onto TiC_5H_5^+ complex. (c) and (d) give the deformation electron density of $\text{TiC}_5\text{H}_5^+(\text{H}_2)_5$ and the LUMO orbital of $\text{TiC}_5\text{H}_5^+(\text{H}_2)_4$, respectively. The isovalue equals $0.02 \text{ e}/\text{\AA}^3$.

C. Hydrogen adsorption on TiC_5H_5^+

The equilibrium geometry of the $\text{TiC}_5\text{H}_5^+(\text{H}_2)_5$ complex is shown in Fig. 1 (b₃). Generally for most transition metals, due to significant charge transfer, the first H_2 molecule is found to dissociate on the complex and bind atomically to metal atoms.¹ Accordingly, the first H_2 molecule is adsorbed dissociatively on the TiC_5H_5 complex with the distance between the two H atoms being 3.11 \AA which agrees well with Kiran's results.¹⁷ However, in the case of the TiC_5H_5^+ complex, the first H_2 has been found to bind in molecular form to the Ti atom. The bond length of the H_2 molecule is 0.83 \AA . Interestingly, even though, in our calculations, the distance between the two H atoms is set to 3 \AA for the initial configuration of $\text{TiC}_5\text{H}_5^+(\text{H}_2)$, the two H atoms approach each other and finally form an H_2 molecule. In order to understand the nature of the different bondings between TiC_5H_5 and TiC_5H_5^+ with the first H_2 , the frontier orbitals have been characterized. The HOMO and LUMO of TiC_5H_5^+ interacting with H_2 are shown in Figs. 4(a) and 4(b). As mentioned above, the HOMO of TiC_5H_5 has predominant $3d$ and $4s$ characteristics and matches the symmetry of the σ^* orbital of H_2 . The favorable HOMO-LUMO overlap leads to the dissociation of the molecule. It can be shown from Mulliken atomic-charge analysis that each H atom receives about 0.2 electrons in $\text{TiC}_5\text{H}_5(2\text{H})$. Additional hydrogen molecules do not dissociate and are adsorbed in molecular form around the Ti atom.¹⁷ In spite of having enough space available for a fifth hydrogen molecule to bind, attempts to attach it failed. In contrast, it is energetically favorable to add a fifth H_2 molecule at the top site [Fig. 1 (b₃)] of the Ti atom in the $\text{TiC}_5\text{H}_5^+(\text{H}_2)_4$ complex, with a binding energy of 0.35 eV . The Ti-H distance for the fifth H_2 is 2.26 \AA , and the H-H bond length is 0.76 \AA which is about 0.06 \AA shorter than for the other four H-H bond lengths. All attempts to bind a sixth H_2 molecule failed, as expected, due to the limit of the 18-

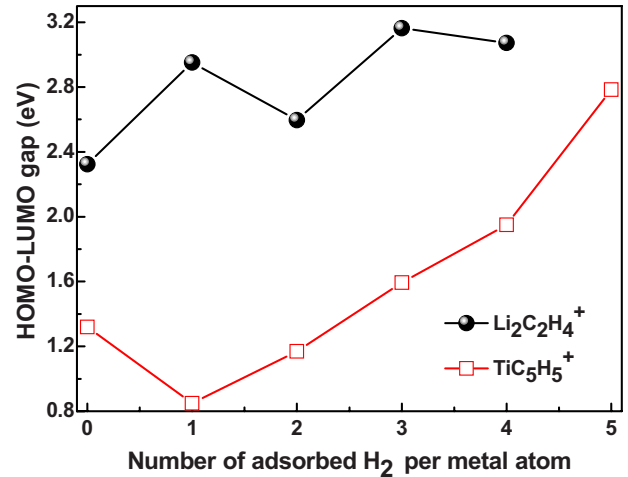


FIG. 5. (Color online) Energy gaps between the HOMO and LUMO for $\text{Li}_2\text{C}_2\text{H}_4^+$ and TiC_5H_5^+ complexes with successive additions of H_2 molecules.

electron rule. Nevertheless, adsorption of five hydrogen molecules corresponds to $8.1 \text{ wt } \%$ hydrogen, which is higher than the hydrogen wt % of 6.6 in the $\text{TiC}_5\text{H}_5(\text{H}_2)_4$ complex.¹⁷

To obtain insight into the nature of the Ti- H_2 bonding, we analyzed the deformation of the electron density of this complex, which was calculated as the difference between the total complex electron density and the density of the isolated atoms. The plot of the deformation electron density exhibits the localized characteristics of H-H bonds [Fig. 4(c)]. The electron back donation from the d orbital of Ti to the antibonding hydrogen s orbital can be found. The remaining two d orbitals (d_{xy} and $d_{x^2-y^2}$), which are parallel to the carbon framework, interact with both bonding and antibonding with respect to the four planar H_2 molecules. A close analysis of the LUMO [Fig. 4(d)] of $\text{TiC}_5\text{H}_5^+(\text{H}_2)_4$ reveals that the d_{z^2} orbital, perpendicular to the carbon framework, is responsible for the binding between the last H_2 molecule and the TM atom. The relative weakness of this bond stems from the large polarization of the d molecular orbital toward the carbon ring. The effective charge of the metal atom, irrespective of the organic template, varies from positive to negative depending on the number of hydrogen atoms bound to it. We studied the Mulliken charge of the Ti atom as a function of the number of H_2 molecules added to it and found that when the fourth and fifth H_2 adsorbed onto it, the Ti atom carried -0.19 and -0.42 electrons, respectively.

D. Kinetic stability and hydrogen desorption

In order to test the kinetic stability of the above hydrogen coated metal-organic systems, we have plotted in Fig. 5 the HOMO-LUMO gaps as a function of the number of adsorbed hydrogen molecules. In particular, the HOMO-LUMO gap of the $\text{Li}_2\text{C}_2\text{H}_4^+(\text{H}_2)_8$ complex is 3.1 eV , which is comparable to that of C_{60} . For $\text{Ti}(\text{C}_5\text{H}_5)(\text{H}_2)_n$, we note that the energy gap noticeably decreases after addition of the first H_2 molecule and remains relatively large as subsequent hydrogen molecules attach until the 18-electron rule is satisfied.

TABLE I. Calculated energy gains ΔE_n (eV) by successive additions of H_2 molecules to organometallic complexes and average binding energy per H_2 , $\overline{\Delta E}$.

Complex	$n=1$	$n=2$	$n=3$	$n=4$	$n=5$	$\Delta E(\text{eV}/H_2)$
$Li_2(C_2H_4)(H_2)_n^a$						0.24
$Li_2(C_2H_4)^+(H_2)_n$	0.28	0.24	0.15	0.43		0.28
$Ti(C_5H_5)(H_2)_n^b$	1.36	0.51	0.45	0.56		0.72
$Ti(C_5H_5)^+(H_2)_n$	0.56	0.61	0.92	0.80	0.35	0.65

^aCalculated with VASP (Vienna *Ab-initio* Simulation Package) code in Ref. 16.

^bCalculated with DMol³ package in Ref. 17.

An ideal storage system would not only be kinetically stable but would also involve molecular adsorption of hydrogen with a binding-energy intermediate between that of physisorption and chemisorption. The energy gains ΔE by successive additions of H_2 molecules to $M(C_aH_b)$ ($a=2$, $b=4$, $M=Li$; $a=5$, $b=5$, $M=Ti$) complexes were calculated using the formula

$$\Delta E_n = E[MC_aH_b(H_2)_n] - E[MC_aH_b(H_2)_{n-1}] - E[H_2] \quad (2)$$

From Eq. (2), the average binding energy per H_2 molecule was computed using

$$\overline{\Delta E} = n_{\max}^{-1} \sum \Delta E_i. \quad (3)$$

Our calculated values of ΔE_n and the average binding energies are summarized in Table I. For $Li_2(C_2H_4)^+(H_2)_n$, the first two consecutive binding energies are close to their average value due to the Li- H_2 binding interaction being close to physisorption. The average binding energy for $Ti(C_5H_5)(H_2)_n$ is quite large due to the strong binding of the first H_2 in the form of a dihydride. Owing to the weak bond between the fifth H_2 molecule and $Ti(C_5H_5)^+(H_2)_4$, the magnitude of ΔE is larger for the nonionic complex than for the ionic one. On the other hand, the opposite is true for the Li-based complex.

Having discussed binding energies we now estimate the desorption temperature T_D using the van't Hoff equation¹⁶

$$T_D = \frac{E_b}{k_B} \left(\frac{\Delta S}{R} - \ln p \right)^{-1} \quad (4)$$

written in terms of E_b , the Boltzmann constant k_B , the change in the H_2 entropy from gas to liquid phase ΔS , the gas constant R , and the equilibrium pressure of 1 atm. Using ΔS from Ref. 33 and the average binding energy from Table I, we can estimate the average desorption temperature T_D . By using the binding energies of the first and last H_2 molecules to be adsorbed by the metal atom, we are also able to deduce the lowest (T_{D_L}) and highest (T_{D_H}) temperature for onset of the desorption and full discharge of hydrogen from the medium. In the case of $Li_2(C_2H_4)^+(H_2)_n$, the estimated T_D , T_{D_L} , and T_{D_H} for the desorption of H_2 are 357, 357, and 548 K. For $Ti(C_5H_5)^+(H_2)_n$, the corresponding values are 715, 830, and 447 K.

IV. CONCLUSIONS

In conclusion, using all-electron DFT-GGA calculations, a fundamental study of the interaction and kinetic stability of H_2 molecule adsorption on $Li_2C_2H_4^+$ and $TiC_5H_5^+$ complexes has been performed. These charged templates are prevented from clustering and can bind Li and Ti with comparable and significant chemisorption energy. In particular, we have shown that $Li_2C_2H_4^+$ can store up to 27.5 wt % of hydrogen. The average binding energy of the H_2 molecule is found to be 0.28 eV. This not only meets the gravimetric density target set by the (U.S.) Department of Energy for the year 2015 but the binding energy is also ideal for the system to operate under ambient thermodynamic conditions. The positively charged C_5H_5 increases the charge transferred from the metal atom to the organic molecule and the bonding between them is strong. In particular, the first H_2 adsorbs in molecular form on the $TiC_5H_5^+$, while it is adsorbed dissociatively on the TiC_5H_5 complex. The bonding mechanism between the Ti atom and the first H_2 in $TiC_5H_5(2H)$ has also been presented; the favorable overlap of HOMO of TiC_5H_5 and LUMO of H_2 leads to the dissociation of the H_2 molecule. We can deduce that controlling the charge state of the metal-organic molecules and decreasing charge transfers between transition-metal atoms and H_2 may prevent the breaking of the hydrogen-hydrogen bond in H_2 . The maximum retrievable hydrogen uptake is predicted as 8.1 wt % for the $TiC_5H_5^+(H_2)_5$ complex based on the 18-electron rule. The resulting binding energies of the hydrogen molecules to the transition-metal atom in the complex are intermediate between physisorption and chemisorption energies. We anticipate that the theoretical results here will provide a useful reference for understanding the mechanism of H_2 interacting with charged complexes and the search for new hydrogen storage media.

ACKNOWLEDGMENTS

We would like to thank N. E. Davison for his help with the language. This work was supported by the National Science Foundation of China under Grant No. 10774148, the special Funds for Major State Basic Research Project of China (973) under Grant No. 2005CB623603, Knowledge Innovation Program of the Chinese Academy of Sciences, and Director Grants of CASHIPS. Part of the calculations were performed in the Center for Computational Science of CASHIPS and the Shanghai Supercomputer Center.

*cslu@theory.issp.ac.cn

†Corresponding author; zzeng@theory.issp.ac.cn

- ¹L. Schlapbach and A. Züttel, *Nature (London)* **414**, 353 (2001).
- ²B. C. H. Steele and A. Heinzl, *Nature (London)* **414**, 345 (2001).
- ³R. Coontz and B. Hanson, *Science* **305**, 957 (2004).
- ⁴G. W. Crabtree, M. S. Dresselhaus, and M. V. Buchanan, *Phys. Today* **57** (12), 39 (2004).
- ⁵A. Züttel, *Mater. Today* **6** (9), 24 (2003).
- ⁶<http://www.eere.energy.gov/hydrogenandfuelcells/mypp/>
- ⁷S. H. Jhi and Y. K. Kwon, *Phys. Rev. B* **69**, 245407 (2004).
- ⁸M. Yoon, S. Yang, E. Wang, and Z. Zhang, *Nano Lett.* **7**, 2578 (2007).
- ⁹K. R. S. Chandrakumar and S. K. Ghosh, *Nano Lett.* **8**, 13 (2008).
- ¹⁰Y. F. Zhao, Y. H. Kim, A. C. Dillon, M. J. Heben, and S. B. Zhang, *Phys. Rev. Lett.* **94**, 155504 (2005).
- ¹¹T. Yildirim, J. Iniguez, and S. Ciraci, *Phys. Rev. B* **72**, 153403 (2005); T. Yildirim and S. Ciraci, *Phys. Rev. Lett.* **94**, 175501 (2005).
- ¹²Y. H. Kim, Y. F. Zhao, A. Williamson, M. J. Heben, and S. B. Zhang, *Phys. Rev. Lett.* **96**, 016102 (2006).
- ¹³Q. Sun, P. Jena, Q. Wang, and M. Marquez, *J. Am. Chem. Soc.* **128**, 9741 (2006).
- ¹⁴H. Lee, W. I. Choi, and J. Ihm, *Phys. Rev. Lett.* **97**, 056104 (2006); H. Lee, W. I. Choi, M. C. Nguyen, M. H. Cha, E. Moon, and J. Ihm, *Phys. Rev. B* **76**, 195110 (2007).
- ¹⁵M. Yoon, S. Yang, C. Hicke, E. Wang, D. Geohegan, and Z. Zhang, *Phys. Rev. Lett.* **100**, 206806 (2008).
- ¹⁶E. Durgun, S. Ciraci, W. Zhou, and T. Yildirim, *Phys. Rev. Lett.* **97**, 226102 (2006); W. Zhou, T. Yildirim, E. Durgun, and S. Ciraci, *Phys. Rev. B* **76**, 085434 (2007).
- ¹⁷B. Kiran, A. K. Kandalam, and P. Jena, *J. Chem. Phys.* **124**, 224703 (2006).
- ¹⁸P. F. Weck and T. J. D. Kumar, *J. Chem. Phys.* **126**, 094703 (2007).
- ¹⁹D. Michael and P. Mingos, *J. Organomet. Chem.* **635**, 1 (2001).
- ²⁰A. B. Phillips and B. S. Shivaram, *Phys. Rev. Lett.* **100**, 105505 (2008).
- ²¹G. J. Kubas, R. R. Ryan, B. I. Swanson, P. J. Vergamini, and H. J. Wasserman, *J. Am. Chem. Soc.* **106**, 451 (1984).
- ²²R. H. Crabtree, *The Organometallic Chemistry of the Transition Metals*, 3rd ed. (Wiley, New York, 2001).
- ²³W. Kohn and L. J. Sham, *Phys. Rev.* **140**, A1133 (1965).
- ²⁴M. Schluter and L. J. Sham, *Phys. Today* **35** (2), 36 (1982).
- ²⁵J. P. Perdew, K. Burke, and M. Ernzerhof, *Phys. Rev. Lett.* **77**, 3865 (1996).
- ²⁶B. Delley, *J. Chem. Phys.* **113**, 7756 (2000).
- ²⁷A. Hazra and M. Nooijena, *J. Chem. Phys.* **122**, 204327 (2005).
- ²⁸M. Shiotani, Y. Nagata, and J. Sohma, *J. Am. Chem. Soc.* **106**, 4640 (1984).
- ²⁹R. S. Mulliken, *Phys. Rev.* **74**, 736 (1948).
- ³⁰H. J. Koehler and H. Lischka, *J. Am. Chem. Soc.* **101**, 3479 (1979).
- ³¹B. Delley, *J. Chem. Phys.* **92**, 508 (1990).
- ³²B. K. Rao and P. Jena, *Europhys. Lett.* **20**, 307 (1992).
- ³³*Handbook of Chemistry and Physics*, 75th ed., edited by D. R. Lide (CRC, New York, 1994).